Loss of Hepatocyte Growth Factor/c-Met Signaling Pathway Accelerates Early Stages of *N*-nitrosodiethylamine–Induced Hepatocarcinogenesis

Taro Takami, Pal Kaposi-Novak, Koichi Uchida, Luis E. Gomez-Quiroz, Elizabeth A. Conner, Valentina M. Factor, and Snorri S. Thorgeirsson

Laboratory of Experimental Carcinogenesis, Center for Cancer Research, National Cancer Institute, NIH, Bethesda, Maryland

Abstract

Hepatocyte growth factor (HGF) has been reported to have both positive and negative effects on carcinogenesis. Here, we show that the loss of c-Met signaling in hepatocytes enhanced rather than suppressed the early stages of chemical hepatocarcinogenesis. c-Met conditional knockout mice (*c-met*$^{fl/fl}$, AlbCre$^{+/-}$; MetLivKO) treated with *N*-nitrosodiethylamine developed significantly more and bigger tumors and with a shorter latency compared with control (*w/w*, AlbCre$^{+/-}$; Cre-Ctrl) mice. Accelerated tumor development was associated with increased rate of cell proliferation and prolonged activation of epidermal growth factor receptor (EGFR) signaling. MetLivKO livers treated with *N*-nitrosodiethylamine also displayed elevated lipid peroxidation, decreased ratio of reduced glutathione to oxidized glutathione, and up-regulation of superoxide dismutase 1 and heat shock protein 70, all consistent with increased oxidative stress. Likewise, gene expression profiling done at 3 and 5 months after *N*-nitrosodiethylamine treatment revealed up-regulation of genes associated with cell proliferation and stress responses in c-Met mutant livers. The negative effects of c-Met deficiency were reversed by chronic p.o. administration of antioxidant *N*–acetyl–L-cysteine. *N*–acetyl–L-cysteine blocked the EGFR activation and reduced the *N*-nitrosodiethylamine–initiated hepatocarcinogenesis to the levels of Cre-Ctrl mice. These results argue that intact HGF/c-Met signaling is essential for maintaining normal redox homeostasis in the liver and has tumor suppressor effect(s) during the early stages of *N*-nitrosodiethylamine–induced hepatocarcinogenesis. [Cancer Res 2007;67(20):9844–51]

Introduction

c-Met, the only known high-affinity receptor for hepatocyte growth factor (HGF; ref. 1, 2), was originally discovered as an oncogene through its ability to induce transformation of NIH3T3 cells (3). The mature form of c-Met consists of a 50-kDa extracellular α chain and a 145-kDa transmembrane β chain containing a tyrosine kinase catalytic domain essential for downstream signaling (4–6). The significance of the HGF/Met signaling pathway as a major regulator of hepatocyte proliferation, survival, and motility is well established (7). Gene targeting experiments showed that this signaling system is required during development. Mice lacking either HGF (8) or c-Met (9) die at midgestation with multiple abnormalities including underdeveloped liver. In addition to being of central importance for embryogenesis and tissue regeneration (10), there is strong evidence that HGF/c-Met signaling controls invasive growth and metastasis in a variety of cancers, including hepatocellular carcinoma (HCC; refs. 11–15).

Nevertheless, experimental mouse models of human liver cancer have revealed that the net outcome of HGF/c-Met activation could be both stimulation and inhibition of hepatocarcinogenesis. For example, transgenic mice expressing HGF driven by the metallothionein promoter developed liver tumors, including HCC albeit with a low frequency and a long latency (14). Alternatively, transgenic mice expressing HGF under control of the albumin promoter did not form liver tumors (16), and transgenic coexpression with HGF suppressed both c-Myc (17) and transforming growth factor-α (TGF-α)–driven (18) hepatocarcinogenesis in double transgenic mice. The cell culture studies have also shown opposite effects of HGF/c-Met on cancer cell growth. Thus, HGF can either increase cell survival (19–21) or inhibit cell growth and induce apoptosis in a variety of cancer cell lines, including HCC and transformed rat liver epithelial cell lines (22–24).

To mechanistically address a role for c-Met in liver carcinogenesis, we used a hepatocyte specific *c-met* conditional knockout (MetLivKO) mouse model generated in our laboratory (25). In these mice, exon 16 of *c-met* gene, which codes for a critical ATP-binding site in the intracellular tyrosine kinase domain (26), was deleted in postnatal hepatocytes by crossing the *c-met*$^{fl/fl}$ mice with Albumin-Cre transgenic mice (27). Under physiologic conditions, MetLivKO livers showed no obvious morphologic or functional abnormalities. Nonetheless, c-Met deleted hepatocytes isolated from the intact livers showed reduced cellular migration and increased adhesion and stress fiber formation, consistent with the postulated roles for HGF/c-Met signaling (15, 25). More significantly, a prolonged absence of c-Met signaling in hepatocytes caused marked metabolic alterations and compensatory up-regulation of cytoprotective transcription factors, such as nuclear factor [erythroid-derived–like 2 (Nrf2)] and its numerous downstream targets (15).

In this study, we used a well characterized model of *N*-nitrosodiethylamine–induced hepatocarcinogenesis to induce liver tumor development (28). We found that rather than delay course of tumor formation, loss of c-Met in hepatocytes greatly increased susceptibility to *N*-nitrosodiethylamine–induced hepatocarcinogenesis. The tumor promoting effect of c-Met deficiency was associated with disruption of redox homeostasis and was prevented by a long-term feeding with the antioxidant *N*–acetyl–L-cysteine. These results assign an important new function to c-Met in the maintenance of tissue homeostasis and define c-Met signaling as an essential component of the tumor-suppressing machinery in the adult liver.

Note: Supplementary data for this article are available at Cancer Research Online (http://cancerres.aacrjournals.org/).

Requests for reprints: Snorri S. Thorgeirsson, Laboratory of Experimental Carcinogenesis, National Cancer Institute, NIH, Building 37, Room 4146A, Bethesda, MD 20892-4262. Phone: 301-496-5688, ext. 204; Fax: 301-496-0734; E-mail: snorri_s_thorgeirsson@nih.gov.

doi:10.1158/0008-5472.CAN-07-1905

Materials and Methods

Mice. MetLivKO (*c-met*$^{fl/fl}$, AlbCre$^{+/-}$) mice were described previously (25). Cre-Ctrl (*w/w*, AlbCre$^{+/-}$) or *c-met*$^{fl/fl}$ mice were used as controls as indicated. All mice were maintained in specific pathogen-free housing and cared for in accordance with the NIH Guide for the Care and Use of Laboratory Animals.

***N*-nitrosodiethylamine hepatocarcinogenesis and *N*–acetyl–L-cysteine treatment.** Mice received a single i.p. injection of 10 μg/g body weight of *N*-nitrosodiethylamine (Sigma-Aldrich, Inc.) at 14 days of age. Livers were examined at 3, 5, 6, 7, and 8 months. Additional cohorts of Cre-Ctrl and MetlivKO mice were chronically subjected to p.o. administration of 80 mmol/L *N*–acetyl–L-cysteine (Sigma-Aldrich) beginning at mating. The offspring continued to receive *N*–acetyl–L-cysteine-supplemented water over the interval of 3 months after *N*-nitrosodiethylamine exposure at 2 weeks of age. There was no reduction in the number of pups per litter in either genotype suggesting that *N*-acetyl-L-cysteine was not toxic during embryo and postnatal development.

Histology, immunohistochemistry, and TUNEL assay. Livers were fixed in 10% neutral formalin o/n at 4°C. Paraffin sections (5 μm) were stained with H&E for histology and quantification of hepatic lesions graded as foci, adenomas, or carcinomas as defined previously (29). The areas occupied by tumors were measured using ImageJ software (NIH). Immunohistochemical staining was carried out by using the avidin-biotin complex method staining kit (Vector Laboratories). Anti-Ki67 (clone TEC-3; DakoCytomation) was used at 1:100 dilution. TUNEL staining was done using the ApopTag Plus Peroxidase *In situ* Apoptosis Detection kit (S7101; Chemicon) according to the manufacturer's protocol. Sections were counterstained with hematoxylin (Vector Laboratories).

Western blotting. Total and nuclear proteins were isolated from frozen liver tissue with T-PER or NE-PER (Pierce Biotechnology) extraction reagents, respectively, containing 1% Halt Protease Inhibitor Cocktail (Pierce Biotechnology), 100 mmol/L sodium fluoride, 1 mmol/L phenylmethylsulfonyl fluoride, and 50 mmol/L sodium orthovanadate according to the manufacturer's protocol. One hundred micrograms of total protein or 25 μg of nuclear protein measured using bicinchoninic acid protein assay kit (Pierce Biotechnology) were separated on SDS-polyacrylamide gels (Invitrogen), transferred to polyvinylidene difluoride membrane (Invitrogen), and probed with commercially available antibodies (see Supplementary Materials and Methods). Membranes were incubated with the appropriate horseradish peroxidase (HRP)–conjugated secondary antibody and immunoreactive bands identified with ECL-Plus Western blotting detection reagents (GE Healthcare Bio-Sciences Corp.). Equal loading was assessed by probing the same membranes with actin Ab-5 antibody (NeoMarker) or in specified cases staining the gel using GelCode Blue Stain (Pierce Biotechnology).

RNA isolation. Total RNA was isolated from frozen liver tissue with TRIzol reagent (Invitrogen) according to the manufacture's instructions. Total RNA (2.0 μg) was reverse transcribed into first strand cDNA using oligo(dT) primers with the SuperScript First Strand Synthesis System for reverse transcription–PCR (RT-PCR; Invitrogen). PCR was done using Platinum PCR SuperMix (Invitrogen) and the specific primers for α-fetoprotein (AFP), EGFR, and glyceraldehyde-3-phosphate dehydrogenase (GAPDH; see Supplementary Materials and Methods for primer sequences). PCR products were resolved on 2% agarose gels and visualized by ethidium bromide staining.

Genomic DNA isolation. Six focal lesions and 20 full blown HCCs with corresponding surrounding liver tissues were isolated from frozen sections by laser capture microdissection using a Leica LMD6000 (Leica Microsystems, Inc.) at 5 and 8 months after *N*-nitrosodiethylamine treatment, respectively. Genomic DNA was extracted from microdissected areas using REDExtract-N-Amp Tissue PCR kit (Sigma-Aldrich). PCR was done using REDExtract-N-Amp PCR Reaction Mix (Sigma-Aldrich) and specific primers for the *c-met* floxed and deleted alleles and cre recombinase (see Supplementary Materials and Methods for specific primer sequences). PCR products were separated on 2% agarose gel and visualized by ethidium bromide staining.

Lipid peroxidation assay. Lipid peroxidation was assayed by the production of thiobarbituric acid–reactive components using spectrophotometry as described by Buege and Aust (30).

Reduced glutathione and oxidized glutathione determination by high performance liquid chromatography. Reduced glutathione (GSH) and oxidized glutathione (GSSG) content were determined by high performance liquid chromatography (HPLC) as described by Farris and Reed (31) with some modifications. Briefly, frozen liver tissues were collected in 1 mL of 10% perchloric acid (Sigma-Aldrich), sonicated, and centrifuged at 5,000×*g* for 5 min at 4°C. After removal of the supernatants, 100 mmol/L iodoacetic acid (Sigma-Aldrich) in 0.2 mmol/L m-cresol (Sigma-Aldrich) was added to each sample and GSH/GSSG solution standards, and the pH was adjusted to 9.0. Samples and standards were incubated in the dark for 1 h followed by the addition of 1 mL of 1% 1-fluoro-2,4-dinitrobenzene (Sigma-Aldrich) in 100% HPLC grade ethanol. *N*-2,4-dinitrophenol (DNP; 100 μL) derivatives were injected into the loop of the HPLC system (Waters) and separated on a 3-aminopropyl column (5 μm; 4.6 mm × 20 cm; Custom LC). Eluted *N*-DNP derivatives were measured by UV detection at 365 nm.

Microarray analysis. For microarray analysis, total RNA was isolated from snap-frozen whole liver samples using the CsCl gradient centrifugation method as described previously (15). The mouse MEEBO library containing 38,467 oligonucleotides among them 30,125 constitutive genomic probes and 4,201 alternatively spliced probes was purchased from Illumina, whereas the microarrays were manufactured in the Advanced Technology Center of the National Cancer Institute. The cDNA synthesis, fluorescent labeling of the samples, and array hybridization were done following the standard procedures (15). Expression profiling was conducted on five animals from each genotype per time point. Total RNA pooled from five wild-type B6/129 strain mouse livers was used as universal hybridization reference. All experiments were done in duplicates following a dye-swapping design. Arrays were scanned with a GenePix 4000A scanner (Axon Instruments, Ltd.) in a way to achieve optimal signal intensity at both channels with <1% saturated spots. After excluding the invalid features, all arrays were normalized to the 50th percentile of the median signal intensity using the mAdb data analysis suite.[1] Unsupervised cluster analysis was done with the Cluster and TreeView programs.[2] The BRB ArrayTools V3.3.0 software package (Biometric Research Branch, National Cancer Institute)[3] was used for the supervised comparison. Differentially expressed genes were selected using a univariate two-sample *t* test ($P < 0.001$) with a random variance model (15). Functional classification of the significant genes was based on the gene ontology annotations.[4]

Statistical analysis. In the remaining comparisons, statistical significance was determined with a Student's *t* test. Results are presented as the mean ± SE, and differences were assumed significant at $P < 0.05$.

Results

c-Met deficiency promotes *N*-nitrosodiethylamine–induced hepatocarcinogenesis. The kinetics of tumor development in MetLivKO livers after *N*-nitrosodiethylamine treatment was assessed by three factors: incidence, size, and multiplicity. In the absence of c-Met signaling in hepatocytes, tumor appeared more rapidly than in Cre-Ctrl mice (Fig. 1). At 5 and 6 months after *N*-nitrosodiethylamine treatment, 56% (5 of 9; $P < 0.05$) and 100% (9 of 9; $P < 0.05$) of MetLivKO mice formed tumors versus 11% (1 of 9) and 44% (4 of 9) of Cre-Ctrl mice, respectively (Fig. 1*A*). In addition, c-Met–deficient livers displayed significantly larger lesions and produced more foci and tumors than *N*-nitrosodiethylamine–initiated Cre-Ctrl livers (Fig. 1*B–D*). The tumor incidence in mice homozygous for a floxed

[1] http://nciarray.nci.nih.gov/
[2] http://rana.lbl.gov/EisenSoftware.htm
[3] http://linus.nci.nih.gov/BRB-ArrayTools.html
[4] www.geneontology.org

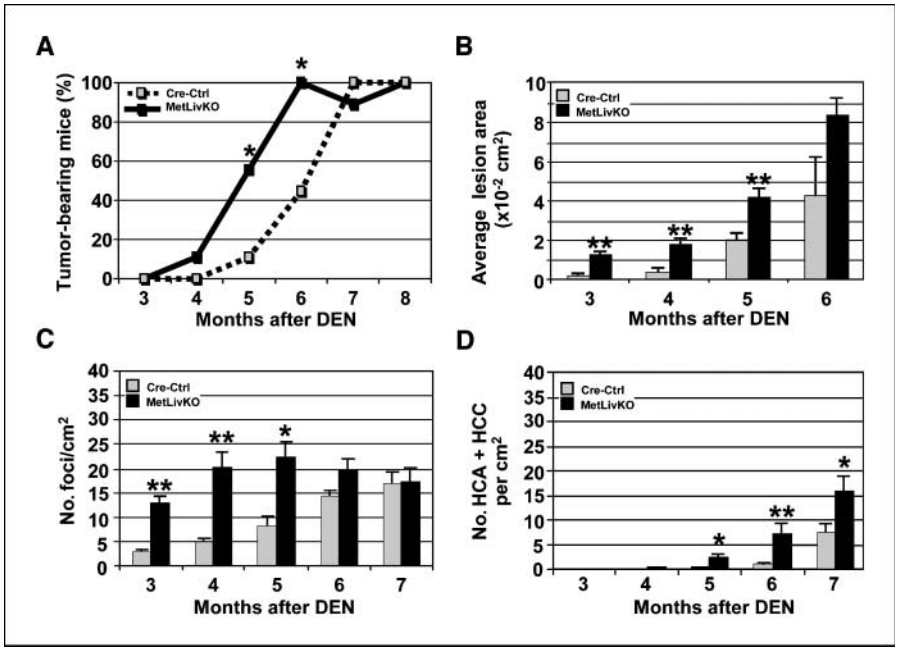

Figure 1. MetLivKO mice are more susceptible than Cre-Ctrl mice to *N*-nitrosodiethylamine–induced hepatocarcinogenesis. *A,* incidence and time course of hepatic lesions from 3 to 8 mo after *N*-nitrosodiethylamine treatment; $n = 9$ for each genotype at each time point. *, $P < 0.05$ compared with Cre-Ctrl mice. *B,* average area occupied by hepatic lesions including foci, adenomas, and carcinomas per square centimeter of the section. *Columns*, mean; *bars*, SE; $n = 6$ for each genotype at each time point. **, $P < 0.01$ compared with Cre-Ctrl mice. Multiplicity of foci (*C*) and multiplicity of tumors (*D*) including adenomas (*HCA*) and HCC per square centimeter. *Columns*, mean; *bars*, SE. *, $P < 0.05$; **, $P < 0.01$ compared with Cre-Ctrl mice.

c-*met*$^{fl/fl}$ allele was lower compared with Cre-Ctrl or c-Met–deficient mice at 8 months after *N*-nitrosodiethylamine treatment (80% versus 100%) in agreement with the known genotoxic effects of Cre-recombinase (32, 33).

Mice of both genotypes developed similar histologic alterations. The predominant tumor phenotype was AFP-positive basophilic cell type typical for *N*-nitrosodiethylamine–induced hepatocarcinogenesis. MetLivKO mice showed an earlier and stronger up-regulation of AFP consistent with a more rapid and extensive tumor growth (Fig. 2*A–B*).

Previously, we have shown that complete deletion of the *c-met* floxed–targeted allele in hepatocytes by Cre-recombinase occurs by 6 weeks of age (25). Since we injected mice with *N*-nitrosodiethylamine at 2 weeks postnatally, there was a possibility that tumors in c-Met conditionally knockout livers could have developed from c-Met–expressing hepatocytes. We therefore

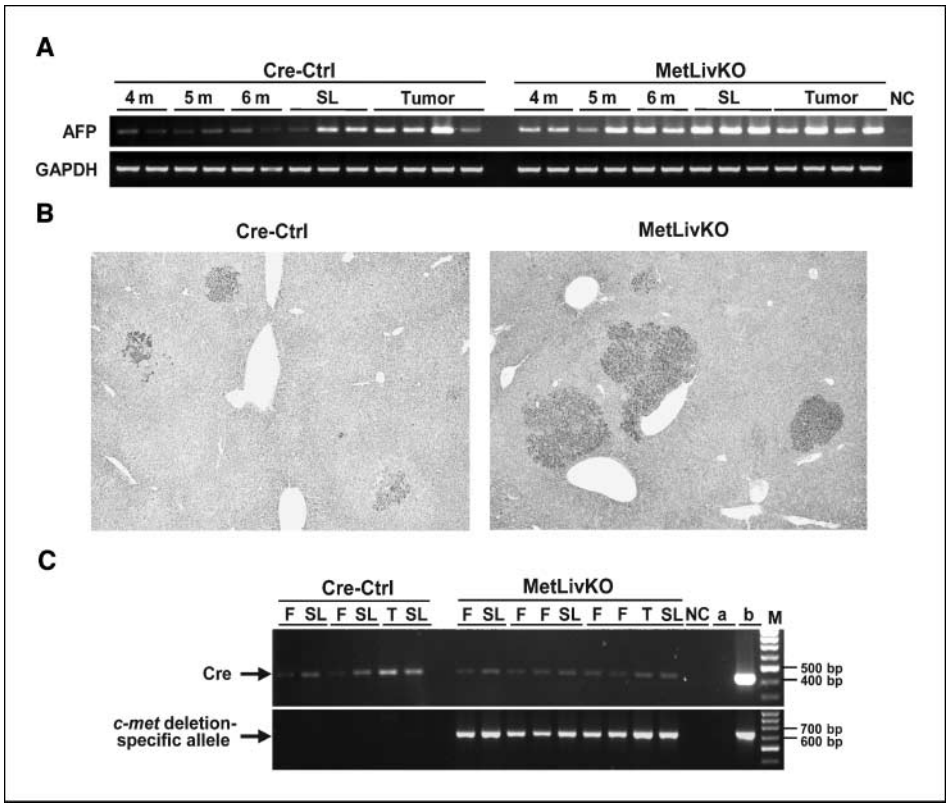

Figure 2. MetLivKO *N*-nitrosodiethylamine–induced tumors express AFP and develop from c-Met–deleted hepatocytes. *A,* expression levels of AFP mRNA by RT-PCR analysis after *N*-nitrosodiethylamine treatment. Tumors and corresponding surrounding livers (*SL*) were extracted from livers at 6 mo after *N*-nitrosodiethylamine treatment. *NC,* negative control. *B,* liver sections at 5 mo after *N*-nitrosodiethylamine treatment immunostained with AFP antibody followed by HRP/3,3′-diaminobenzidine detection. Original magnification, ×25. *C,* PCR analysis of genomic DNA extracted from foci (*F*), HCC (*T*), and corresponding surrounding livers by laser microdissection at 5 and 8 mo after *N*-nitrosodiethylamine treatment, respectively. *Arrows,* PCR fragments corresponding to Cre (412 bp) and the *c-met* deletion–specific allele (650 bp). *NC,* negative control with omission of DNA; *a*, genomic DNA from *c-met*$^{fl/fl}$, AlbCre$^{-/-}$ liver; *b*, genomic DNA from *c-met*$^{fl/fl}$, AlbCre$^{+/-}$ liver; *M*, DNA ladder.

genotyped both early focal lesions and full blown HCC developed in MetLivKO at 5 and 8 months after *N*-nitrosodiethylamine treatment. PCR analysis of genomic DNA extracted from six laser-microdissected focal lesions and 20 HCC showed the presence of the *c-met* deletion-specific allele (650 bp; Fig. 2*C*). These results show that loss of the c-Met function in hepatocytes has contributed to the earlier tumor onset in MetLivKO mice.

MetLivKO tumors display enhanced cell proliferation during early stages of *N*-nitrosodiethylamine–induced hepatocarcinogenesis. Next, we examined whether deregulation of proliferation or apoptosis caused the faster tumor growth in c-Met–deficient livers. There was no significant difference in the apoptotic index between control and mutant livers at 5 months after *N*-nitrosodiethylamine treatment. In contrast, c-Met–deficient tumors showed a considerable increase in the number of proliferating cells. The labeling index, as assessed by Ki-67 immunohistochemistry, was consistently higher in MetLivKO tumors at 5 and 6 months after *N*-nitrosodiethylamine (Fig. 3*A–B*). However, at the advanced tumor stage (8 months after *N*-nitrosodiethylamine), the growth rate was comparable in both genotypes, suggesting that the loss of c-Met function was more critical for the early stages of tumor development.

The high rate of cell proliferation in MetLivKO livers coincided with the activation of EGFR signaling, another key regulator of liver mitogenesis and tumorigenesis (34, 35). Immunoblot analysis using phosphor-specific antibodies revealed an increase in both basal and *N*-nitrosodiethylamine–induced levels of EGFR phosphorylation. This correlated with a strong and sustained activation of EGFR downstream targets, p42/p44 mitogen-activated protein kinase and protein kinase C α/β_{II} (Fig. 3*C*).

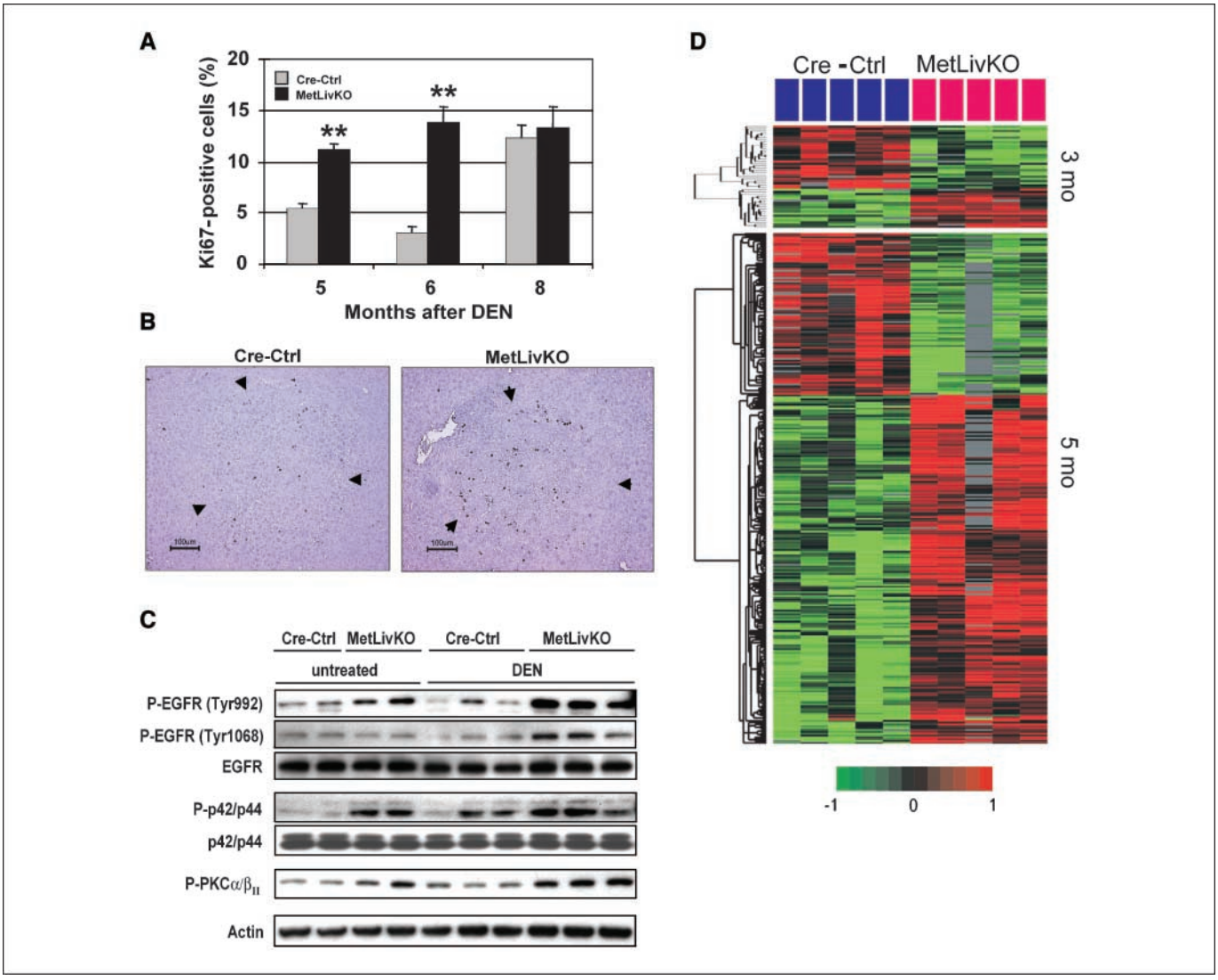

Figure 3. Increased proliferation, EGFR activation, and disregulation of stress response genes in MetLivKO mice after *N*-nitrosodiethylamine. *A,* Ki67 labeling index. *Columns*, frequency of Ki67-positive nuclei at 5, 6, and 8 mo after *N*-nitrosodiethylamine treatment; *bars*, SE; $n = 9$. **, $P < 0.01$ compared with Cre-Ctrl mice. *B,* immunohistochemical staining of Ki67 protein in focal lesions demarcated by arrows. *Scale bar,* 100 μm. *C,* representative Western blot of whole-cell lysates from Cre-Ctrl and MetLivKO livers at 5 mo with and without *N*-nitrosodiethylamine treatment. Antibodies used are indicated. All blots were reprobed with antiactin as a control for loading. *D,* transcription patterns of genes differentially expressed after *N*-nitrosodiethylamine treatment. The two-dimensional heat map is constructed from expression values of 57 and 317 significant genes ($P < 0.001$) at 3 and 5 mo after *N*-nitrosodiethylamine treatment, respectively. The differentially expressed genes were identified by comparing expression levels in the MetLivKO and Cre-Ctrl samples with a two-sample *t* test. *Columns,* individual samples; *rows,* genes. Thus, each cell reflects the $\log_2$ transformed expression ratio of an individual gene in a given sample, as indicated by the color code on the figure.

Table 1. Functional classification of the differentially expressed genes by gene ontology categories

GO class ID	GO classification	Time point (mo)	Observed in selected	Observed/expected	*P*
17114	Wide-spectrum protease inhibitor activity	5	7	73.65	4.13e−104
30106	MHC class I receptor activity	5	15	13.72	2.84e−39
19885	Antigen processing	5	15	12.11	6.97e−34
19883	Antigen presentation	5	15	11.97	1.42e−32
19882	Antigen presentation	5	16	10.02	4.74e−27
30333	Antigen processing	5	15	10	1.51e−24
6968	Cellular defense response	5	15	8.58	2.15e−19
4867	Serine protease inhibitor activity	5	8	7.09	8.52e−10
9611	Response to wounding	5	17	4.29	9.02e−07
4866	Endopeptidase inhibitor activity	5	8	4.55	1.57e−05
30414	Protease inhibitor activity	5	8	4.52	1.73e−05
5830	Cytosolic ribosome	5	5	6.16	1.97e−05
9613	Response to pest/pathogen/parasite	5	20	3.6	4.42e−05
5887	Integral to plasma membrane	5	27	2.21	1.36e−04
5783	Endoplasmic reticulum	3	7	3.73	9.38e−04
3735	Structural constituent of ribosome	5	9	3.12	1.57e−03
5840	Ribosome	5	9	3.07	1.86e−03
4857	Enzyme inhibitor activity	5	8	3.09	3.52e−03
16491	Oxidoreductase activity	3	8	2.79	9.86e−03
9056	Catabolism	3	8	2.77	1.09e−02
16788	Hydrolase activity, acting on ester bonds	3	6	2.8	3.18e−02
6887	Exocytosis	5	5	4.48	6.21e−02

Abbreviation: GO, gene ontology.

Disregulation of genes associated with cell proliferation and stress responses in MetLivKO livers by microarray analysis. To further screen for the alterations caused by *c-met* gene disruption, we did gene expression profile analysis of *N*-nitrosodiethylamine–initiated MetLivKO and Cre-Ctrl livers. Supervised class comparison using a two-sample *t* test identified 57 and 317 differentially expressed genes at 3 and 5 months after *N*-nitrosodiethylamine treatment, respectively ($P < 0.001$; Fig. 3*D*; Supplementary Table S1). Consistent with the higher rate of cell proliferation in MetLivKO tumors (Fig. 3*A*), we found overexpression of several cell cycle–associated genes, including dual specific phosphatase 1 (*Dusp1*) and components of the NADH dehydrogenase α complex (*Ndufa7, Nodufa12*). In addition, functional analysis based on gene ontology classification showed overrepresentation of the ribosomal protein cluster ($P < 0.00002$; observed/expected ratio, O/E = 6.1) in mice lacking *c-met* gene in hepatocytes (Table 1).

Remarkably, the most prominent effect of c-Met deficiency was sustained misregulation of various oxidative stress response genes. At 3 months after *N*-nitrosodiethylamine administration, many genes encoding the metabolic enzymes located in the endoplasmic reticulum ($P < 00093$, O/E = 3.73; Table 1) were invariably up-regulated. Among these were cytochrome P450 oxidases (*Cyp3a13, Cyp3a44, Cyp4f16, Cyp2d13*), the microsomal cytochrome (*Cyb5a*), and the glutamine synthesis enzymes asparagine synthase (*Asns*) and ornithine aminotransferase (*Oat*). Members of this class could contribute to the enhanced production of reactive oxygen species (ROS). The metabolic alterations persisted at the 5 months time point. In addition, the 70-kDa heat shock protein 1B (*Hspa1b*), the 60-kDa *Hspd1*, the glutathione *S*-transferase mu 2 (*Gstm2*), and peroxiredoxin 4 (*Prdx4*) were found to be significantly more abundant in the c-Met conditional knockout livers ($P < 0.001$).

Increased oxidative stress in *N*-nitrosodiethylamine–treated MetLivKO livers. To substantiate the microarray data, we measured the redox status in *N*-nitrosodiethylamine–initiated MetLivKO and control livers. The content of malondialdehyde, the major aldehyde end product of membrane lipid peroxidation, was significantly higher in MetLivKO than in Cre-Ctrl livers at 5 months after *N*-nitrosodiethylamine treatment (Fig. 4*A*). Concomitantly, the ratio of reduced to oxidized glutathione was decreased in MetLivKO livers (Fig. 4*B*). Furthermore, we found increased nuclear translocation of Nrf2 in the untreated c-Met–deficient livers (Fig. 4*C*). The transcription factor Nrf2 regulates the basal and inducible expression of numerous antioxidant and detoxifying genes and is activated by endogenous products of oxidative stress including 4-hydroxynonenal (36). Consistent with this and microarray data, the protein levels of Hsp70 and antioxidant enzymes superoxide dismutase 1 (Sod1) were increased in MetLivKO livers (Fig. 4*D*). Together, these data suggest that the lack of c-Met function in hepatocytes increased oxidative stress.

Antioxidant *N*-acetyl-L-cystein reversed the promoting effect of c-Met deficiency on *N*-nitrosodiethylamine–induced hepatocarcinogenesis. To determine whether an increase in ROS may account for acceleration of *N*-nitrosodiethylamine–initiated hepatocarcinogenesis, we studied the chemopreventive effects of a potent antioxidant *N*-acetyl-L-cysteine. We chose *N*-acetyl-L-cysteine because it can compensate for reduced GSH levels by increasing cysteine pool or acting directly as ROS scavenger, and it has been shown to be effective in suppression of oxidative and genotoxic damage by chemical carcinogens *in vivo* (37). Chronic supplementation with *N*-acetyl-L-cysteine–containing water for 3 months

induced no obvious toxicity as evidenced by clinical observations and gross pathology at necroscopy. There were no significant differences in the food intake as well as the liver/body weight ratios at the end of the study compared with mice receiving normal diet (data not shown).

Strikingly, p.o. *N*-acetyl-L-cysteine administration slowed down the *N*-nitrosodiethylamine–initiated tumor growth in c-Met–deficient livers without affecting Cre-Ctrl hepatocarcinogenesis (Fig. 5*A* and *B*). At 3 months, the average size of focal lesions in MetLivKO mice was reduced >3-fold and reached the levels found in Cre-Ctrl mice. Dietary *N*-acetyl-L-cysteine also decreased the multiplicity of focal lesions in c-Met–deficient livers by 1.8-fold ($P = 0.02$) although not to the same extent as focus size ($P = 0.052$). Retardation of tumor growth was associated with a strong decrease in the levels of EGFR phosphorylation (Fig. 5*C*). Thus, the chronic administration of the antioxidant *N*-acetyl-L-cysteine reversed the c-Met$^{-/-}$ phenotype and defined ROS as a key mediator of the increased susceptibility to *N*-nitrosodiethylamine–induced hepatocracinogenesis in MetLivKO mice.

Discussion

In the present study, we show that hepatocyte-specific deletion of *c-met*$^{fl/fl}$ targeted allele with the Alb-Cre recombinase transgene had a profound effect on liver biology and dramatically increased the susceptibility to *N*-nitrosodiethylamine–induced hepatocarcinogenesis. In the absence of intact HGF/c-Met signaling, tumors developed earlier were bigger and more numerous than in Cre-Ctrl mice.

Interestingly, the loss of c-Met conferred growth advantage to *N*-nitrosodiethylamine–initiated cells at the early, rather than late, stages of hepatocracinogenesis, suggesting that the effects of *c-met* gene disruption may vary depending on the stage of carcinogenesis (Figs. 1 and 3*A*). Previous findings support the critical role for HGF/c-Met signaling at the initiation stage. Thus, administration of HGF caused inhibition of cell proliferation in the preneoplastic lesions positive for glutathione *S*-transferase placental form in the rat model of *N*-nitrosodiethylamine hepatocarcinogenesis (38) while stimulating hepatic DNA synthesis in normal and partially hepatectomized rats (39). Consistent with this, we and others has recently shown that c-Met is required for normal liver regeneration (25, 40, 41). Together, the data support the idea that HGF may elicit the opposing proliferative responses in normal and transformed cells of the same origin (38) and functions to suppress tumor formation by restricting the proliferation of initiated cells during the early stages of *N*-nitrosodiethylamine–induced hepatocarcinogenesis.

There were no apparent differences in apoptosis between c-Met mutant and control tumors implying that disregulation of proliferation is principally responsible for the earlier tumor onset in MetLivKO mice. The increased rate of cell division was associated with the early and enhanced activation of EGFR signaling pathway. EGFR, also known as ERBB1 or HER1, is one of the major regulators of hepatocyte proliferation, which belongs to the ErbB family of transmembrane receptors tyrosine kinases (34). EGF/EGFR pathway has a strong stimulatory effect on hepatoma growth and is frequently overexpressed in human HCC, particular at the more aggressive stage (35). Although the mechanisms underlying increased EGFR signaling may differ, EGFR up-regulation in

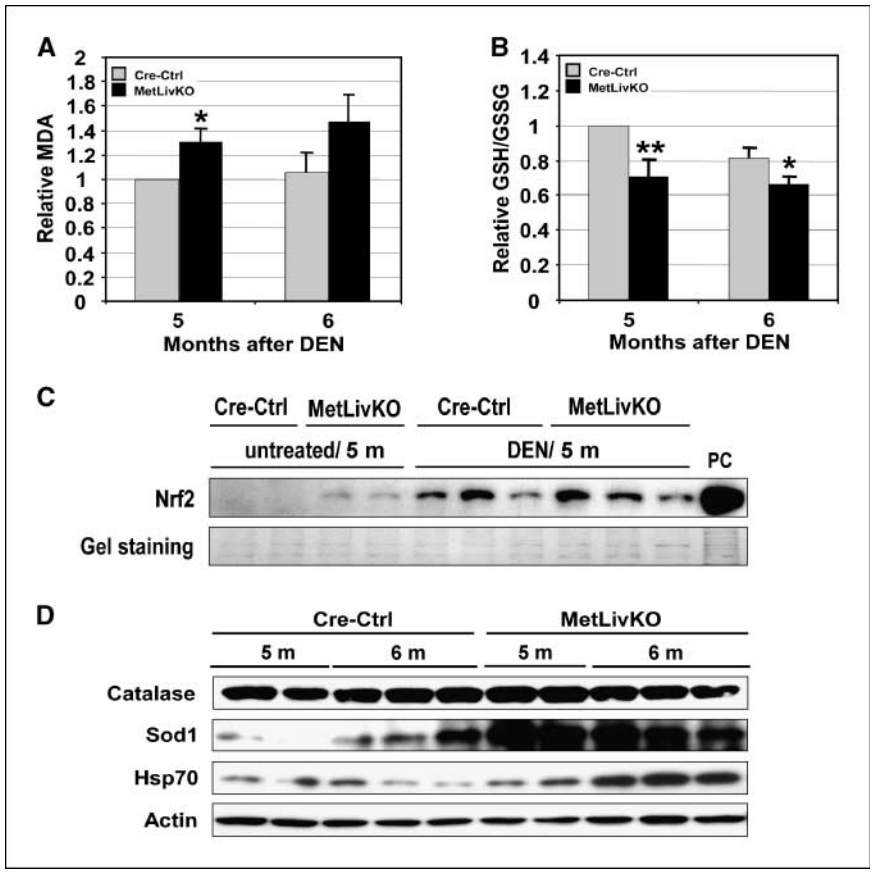

Figure 4. Disruption of redox homestasis in MetLivKO mice. *A,* lipid peroxidation assessed by malondialdehyde (*MDA*) content in Cre-Ctrl and MetLivKO livers at 5 and 6 mo after *N*-nitrosodiethylamine treatment. *Columns*, relative ratios to the mean in Cre-Ctrl at 5 mo; *bars*, SE; $n = 6$ per genotype. *, $P < 0.05$ compared with Cre-Ctrl mice. *B,* the ratio of GSH to GSSG in Cre-Ctrl and MetLivKO livers at 5 and 6 mo after *N*-nitrosodiethylamine treatment. *Columns*, relative ratios to the mean in Cre-Ctrl at 5 mo; *bars,* SD; $n = 3$. *, $P < 0.05$; **, $P < 0.01$ compared with Cre-Ctrl mice. *C,* representative Western blot of nuclear extracts from Cre-Ctrl and MetLivKO livers at 5 mo with and without *N*-nitrosodiethylamine treatment. *PC,* THP-1 nuclear extract as positive control. *D,* representative Western blots of whole lysates from Cre-Ctrl and MetLivKO livers at 5 and 6 mo after *N*-nitrosodiethylamine treatment. Antibodies used are indicated. All blots were reprobed with antiactin as control for loading and membrane transfer.

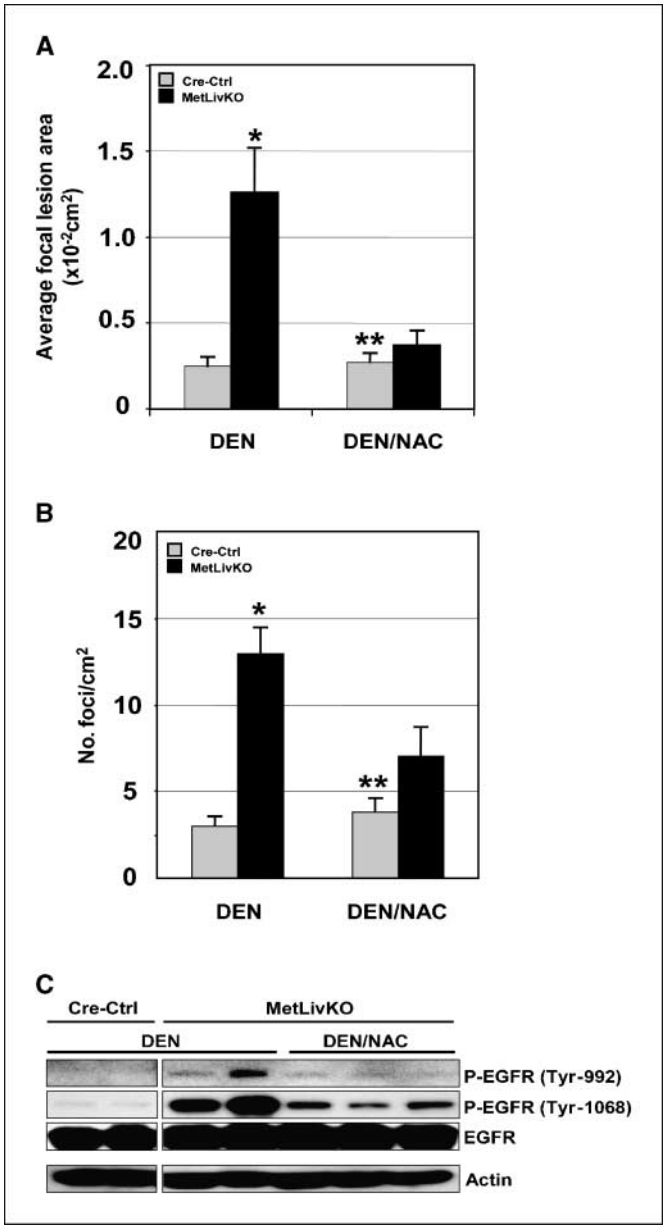

Figure 5. Oral administration of *N*-acetyl-L-cysteine blocked EGFR activation and reduced *N*-nitrosodiethylamine–induced hepatocarcinogenesis in MetLivKO mice. *A,* average area occupied by hepatic lesions per square centimeter of liver section at 3 mo after *N*-nitrosodiethylamine treatment. Cre-Ctrl and MetLivKO mice treated with *N*-nitrosodiethylamine were maintained either on normal diet (*DEN*, nine mice per genotype) or diet supplemented with *N*-acetyl-L-cysteine (*DEN/NAC*, seven mice per genotype). *Columns*, average focal area; *bars*, SE. *, $P = 3.85e{-}05$ compared with Cre-Ctrl/*N*-nitrosodiethylamine and $P = 0.0002$ compared with MetLivKO/*N*-nitrosodiethylamine/*N*-acetyl-L-cysteine mice; **, $P = 0.79$ compared with Cre-Ctrl/*N*-nitrosodiethylamine mice and $P = 0.27$ compared with MetLivKO/*N*-nitrosodiethylamine/*N*-acetyl-L-cysteine mice. *B,* multiplicity of focal lesions in Cre-Ctrl and MetLivKO livers at 3 mo after *N*-nitrosodiethylamine treatment. Cre-Ctrl and MetLivKO mice treated with *N*-nitrosodiethylamine were maintained either on normal diet (*DEN*) or diet supplemented with *N*-acetyl-L-cysteine (*DEN/NAC*). *Columns*, mean number of foci; *bars*, SE; *, $P = 6.04e{-}05$ compared with Cre-Ctrl/*N*-nitrosodiethylamine and $P = 0.02$ compared with MetLivKO/*N*-nitrosodiethylamine/*N*-acetyl-L-cysteine mice; **, $P = 0.44$ compared with Cre-Ctrl/*N*-nitrosodiethylamine mice and $P = 0.052$ compared with MetLivKO/*N*-nitrosodiethylamine/*N*-acetyl-L-cysteine mice. *C,* representative Western blot of whole-cell lysates from Cre-Ctrl and MetLivKO livers at 3 mo after *N*-nitrosodiethylamine treatment with and without *N*-acetyl-L-cysteine supplementation. Antibodies used are indicated. All blots were reprobed with antiactin as a control for loading.

c-Met–deficient tumors might be caused by increased ROS production (42, 43).

Indeed, our data show that the loss of a functional c-Met in hepatocytes promoted a state of chronic oxidative stress. MetLivKO livers displayed increased oxidative damage to lipid, as well as DNA[5] and reduced levels of GSH. We also found up-regulation of a number of the antioxidant genes, including Sod1 and Hsp70 (Fig. 4; Supplementary Table S1) as a compensatory response to ROS exposure. Thus, Hsp70 has been shown to be induced in parallel with a decrease in glutathione content (44) and to provide protection against hydrogen peroxides (45). Up-regulation of Hsp70 has been also found in a c-Myc/TGF-α transgenic model of liver cancer in association with increased ROS production (46, 47). Significantly, intact c-Met–deficient livers exhibited elevated nuclear levels of Nrf2, a key transcription factor protecting against oxidative and xenobiotic stress (Fig. 4*D*; ref. 36). Previously, a profound misregulation of Nrf2 and its numerous target genes related to stress responses or glutathione metabolism has been identified as a part of c-Met–dependent gene expression signature in our microarray study of cultured hepatocytes (15). Remarkably, lack of the intact c-Met signaling not only abolished transcriptional activation of the early response, cytoskeletal, and cell motility–related genes in response to recombinant HGF treatment, but also led to long standing metabolic alterations. Multiple genes responsible for maintaining cellular homeostasis or involved in oxidative stress responses showed constitutively higher level of expression in the c-Met–deficient hepatocytes. Collectively, these results argue that constitutive overexpression of antioxidant genes and phase II detoxification enzyme genes in c-Met–deficient livers may be attributable to a long-term adaptation to prooxidative microenvironment. Nonetheless, the up-regulation of cytoprotective genes in MetLivKO livers may sustain the tolerance to oxidative stress only under normal conditions but fails to shield from an additional oxidative load caused by *N*-nitrosodiethylamine exposure (48, 49).

In support of this contention, the prooxidative effects of c-Met deficiency were rescued by an oral administration of the thiol-containing antioxidant *N*-acetyl-L-cysteine. Chronic dietary supplementation with *N*-acetyl-L-cystein slowed down the growth of *N*-nitrosodiethylamine–initiated focal lesions in MetLivKO livers and reduced hepatocarcinogenesis to the levels of Cre-control livers (Fig. 5). In contrast, the same intake of *N*-acetyl-L-cysteine did not have an effect in Cre-Ctrl mice in agreement with the previous findings in *N*-nitrosodiethylamine–exposed C3H mice (50). The antitumor effect of *N*-acetyl-L-cysteine was associated with inhibition of EGFR phosphorylation, suggesting that activation of alternative signaling pathways evoked by oxidative stress, such as EGFR, may contribute to hepatic oncogenesis. *N*-acetyl-L-cysteine–sensitive suppression of oxidation-mediated carcinogenesis has been described in other mouse models of genetic deficiencies, causing increased ROS production and/or compromised antioxidant defense. Thus, *N*-acetyl-L-cysteine treatment reversed the oxidative DNA damage and the frequency of DNA deletions in Atm (51) as well as in Trp53 knockout mice (52). Likewise, *N*-acetyl-L-cysteine suppressed the compensatory cell proliferation and prevented excessive

[5] Own unpublished observation.

N-nitrosodiethylamine–induced hepatocarcinogenesis in IKKβ-deficient mice by blocking ROS production and prolonged c-Jun-NH_2-kinase activation (53). The chemopreventive effects of *N*-acetyl-L-cysteine lend a strong support to the assumption that the conditional deletion of c-Met in hepatocytes creates a chronic state of oxidative stress whereby contributing to acceleration of *N*-nitrosodiethylamine–induced hepatocarcinogenesis.

In conclusion, this study is the first to report that HGF/c-Met signaling possesses tumor suppressive properties by controlling intracellular redox state and restricting the proliferation of initiated cells. These unexpected findings of tumor-promoting effects of c-Met deficiency may have important implications for the development of therapeutic strategies directed toward c-Met.

Acknowledgments

Received 5/23/2007; revised 8/6/2007; accepted 8/15/2007.

Grant support: Intramural Research Program of the NIH, National Cancer Institute, Center for Cancer Research.

The costs of publication of this article were defrayed in part by the payment of page charges. This article must therefore be hereby marked *advertisement* in accordance with 18 U.S.C. Section 1734 solely to indicate this fact.

We thank Timothy Benjamin, Tanya Hoang, and Anita Ton for their assistance with HPLC analysis, immunohistochemistry, and animal care.

References

1. Bottaro DP, Rubin JS, Faletto DL, et al. Identification of the hepatocyte growth factor receptor as the c-met proto-oncogene product. Science 1991;251:802–4.
2. Cooper CS, Park M, Blair DG, et al. Molecular cloning of a new transforming gene from a chemically transformed human cell line. Nature 1984;311:29–33.
3. Chan AM, King HW, Deakin EA, et al. Characterization of the mouse met proto-oncogene. Oncogene 1988;2:593–9.
4. Furge KA, Zhang YW, Vande Woude GF. Met receptor tyrosine kinase: enhanced signaling through adapter proteins. Oncogene 2000;19:5582–9.
5. Birchmeier C, Birchmeier W, Gherardi E, Vande Woude GF. Met, metastasis, motility and more. Nat Rev Mol Cell Biol 2003;4:915–25.
6. Schmidt C, Bladt F, Goedecke S, et al. Scatter factor/hepatocyte growth factor is essential for liver development. Nature 1995;373:699–702.
7. Comoglio PM. Pathway specificity for Met signalling. Nat Cell Biol 2001;3:E161–2.
8. Li Y, Lal B, Kwon S, et al. The scatter factor/hepatocyte growth factor: c-met pathway in human embryonal central nervous system tumor malignancy. Cancer Res 2005; 65:9355–62.
9. Qian CN, Guo X, Cao B, et al. Met protein expression level correlates with survival in patients with late-stage nasopharyngeal carcinoma. Cancer Res 2002;62:589–96.
10. Matsumoto K, Nakamura T. Hepatocyte growth factor (HGF) as a tissue organizer for organogenesis and regeneration. Biochem Biophys Res Commun 1997; 239:639–44.
11. Corso S, Comoglio PM, Giordano S. Cancer therapy: can the challenge be MET? Trends Mol Med 2005;11: 284–92.
12. Peruzzi B, Bottaro DP. Targeting the c-Met signaling pathway in cancer. Clin Cancer Res 2006; 12:3657–60.
13. Ueki T, Fujimoto J, Suzuki T, Yamamoto H, Okamoto E. Expression of hepatocyte growth factor and its receptor c-met proto-oncogene in hepatocellular carcinoma. Hepatology 1997;25:862–6.
14. Sakata H, Takayama H, Sharp R, Rubin JS, Merlino G, LaRochelle WJ. Hepatocyte growth factor/scatter factor overexpression induces growth, abnormal development, and tumor formation in transgenic mouse livers. Cell Growth Differ 1996;7:1513–23.
15. Kaposi-Novak P, Lee JS, Gomez-Quiroz L, Coulouarn C, Factor VM, Thorgeirsson SS. Met-regulated expression signature defines a subset of human hepatocellular carcinomas with poor prognosis and aggressive phenotype. J Clin Invest 2006;116:1582–95.
16. Shiota G, Wang TC, Nakamura T, Schmidt EV. Hepatocyte growth factor in transgenic mice: effects on hepatocyte growth, liver regeneration and gene expression. Hepatology 1994;19:962–72.
17. Santoni-Rugiu E, Preisegger KH, Kiss A, et al. Inhibition of neoplastic development in the liver by hepatocyte growth factor in a transgenic mouse model. Proc Natl Acad Sci U S A 1996;93:9577–82.
18. Shiota G, Kawasaki H, Nakamura T, Schmidt EV. Characterization of double transgenic mice expressing hepatocye growth factor and transforming growth factor α. Res Commun Mol Pathol Pharmacol 1995;90:17–24.
19. Miyazaki M, Gohda E, Tsuboi S, et al. Human hepatocyte growth factor stimulates the growth of HUH-6 clone 5 human hepatoblastoma cells. Cell Biol Int Rep 1992;16:145–54.
20. Lee HS, Huang AM, Huang GT, et al. Hepatocyte growth factor stimulates the growth and activates mitogen-activated protein kinase in human hepatoma cells. J Biomed Sci 1998;5:180–4.
21. Suzuki A, Hayashida M, Kawano H, Sugimoto K, Nakano T, Shiraki K. Hepatocyte growth factor promotes cell survival from fas-mediated cell death in hepatocellular carcinoma cells via Akt activation and Fas-death-inducing signaling complex suppression. Hepatology 2000;32:796–802.
22. Shiota G, Rhoads DB, Wang TC, Nakamura T, Schmidt EV. Hepatocyte growth factor inhibits growth of hepatocellular carcinoma cells. Proc Natl Acad Sci U S A 1992;89:373–7.
23. Derksen PW, de Gorter DJ, Meijer HP, et al. The hepatocyte growth factor/Met pathway controls proliferation and apoptosis in multiple myeloma. Leukemia 2003;17:764–74.
24. Conner EA, Wirth PJ, Kiss A, Santoni-Rugiu E, Thorgeirsson SS. Growth inhibition and induction of apoptosis by HGF in transformed rat liver epithelial cells. Biochem Biophys Res Commun 1997;236:396–401.
25. Huh CG, Factor VM, Sanchez A, Uchida K, Conner EA, Thorgeirsson SS. Hepatocyte growth factor/c-met signaling pathway is required for efficient liver regeneration and repair. Proc Natl Acad Sci U S A 2004;101: 4477–82.
26. Bladt F, Riethmacher D, Isenmann S, Aguzzi A, Birchmeier C. Essential role for the c-met receptor in the migration of myogenic precursor cells into the limb bud. Nature 1995;376:768–71.
27. Sauer B, Henderson N. Site-specific DNA recombination in mammalian cells by the Cre recombinase of bacteriophage P1. Proc Natl Acad Sci U S A 1988;85: 5166–70.
28. Verna L, Whysner J, Williams GM. N-nitrosodiethylamine mechanistic data and risk assessment: bioactivation, DNA-adduct formation, mutagenicity, and tumor initiation. Pharmacol Ther 1996;71:57–81.
29. Frith CH, Ward JM, Turusov VS. Tumours of the liver. Lyon: IARC Scientific Publications; 1994.
30. Buege JA, Aust SD. Microsomal lipid peroxidation. Methods Enzymol 1978;52:302–10.
31. Fariss MW, Reed DJ. High-performance liquid chromatography of thiols and disulfides: dinitrophenol derivatives. Methods Enzymol 1987;143:101–9.
32. Silver DP, Livingston DM. Self-excising retroviral vectors encoding the Cre recombinase overcome Cre-mediated cellular toxicity. Mol Cell 2001;8:233–43.
33. Loonstra A, Vooijs M, Beverloo HB, et al. Growth inhibition and DNA damage induced by Cre recombinase in mammalian cells. Proc Natl Acad Sci U S A 2001; 98:9209–14.
34. Carver RS, Stevenson MC, Scheving LA, Russell WE. Diverse expression of ErbB receptor proteins during rat liver development and regeneration. Gastroenterology 2002;123:2017–27.
35. Ito Y, Takeda T, Sakon M, et al. Expression and clinical significance of erb-B receptor family in hepatocellular carcinoma. Br J Cancer 2001;84:1377–83.
36. Kobayashi M, Yamamoto M. Molecular mechanisms activating the Nrf2-1 pathway of antioxidant gene regulation. Antioxid Redox Signal 2005;7:385–94.
37. De Flora S, Izzotti A, D'Agostini F, Balansky RM. Mechanisms of N-acetylcysteine in the prevention of DNA damage and cancer, with special reference to smoking-related end-points. Carcinogenesis 2001;22:999–1013.
38. Liu ML, Mars WM, Michalopoulos GK. Hepatocyte growth factor inhibits cell proliferation *in vivo* of rat hepatocellular carcinomas induced by diethylnitrosamine. Carcinogenesis 1995;16:841–3.
39. Webber EM, Godowski PJ, Fausto N. *In vivo* response of hepatocytes to growth factors requires an initial priming stimulus. Hepatology 1994;19:489–97.
40. Borowiak M, Garratt AN, Wustefeld T, Strehle M, Trautwein C, Birchmeier C. Met provides essential signals for liver regeneration. Proc Natl Acad Sci U S A 2004;101:10608–13.
41. Paranjpe S, Bowen WC, Bell AW, Nejak-Bowen K, Luo JH, Michalopoulos GK. Cell cycle effects resulting from inhibition of hepatocyte growth factor and its receptor c-Met in regenerating rat livers by RNA interference. Hepatology 2007;45:1471–7.
42. Adler V, Yin Z, Tew KD, Ronai Z. Role of redox potential and reactive oxygen species in stress signaling. Oncogene 1999;18:6104–11.
43. Meves A, Stock SN, Beyerle A, Pittelkow MR, Peus D. H(2)O(2) mediates oxidative stress-induced epidermal growth factor receptor phosphorylation. Toxicol Lett 2001; 122:205–14.
44. Calabrese V, Testa G, Ravagna A, Bates TE, Stella AM. HSP70 induction in the brain following ethanol administration in the rat: regulation by glutathione redox state. Biochem Biophys Res Commun 2000;269:397–400.
45. Su CY, Chong KY, Owen OE, Dillmann WH, Chang C, Lai CC. Constitutive and inducible hsp70s are involved in oxidative resistance evoked by heat shock or ethanol. J Mol Cell Cardiol 1998;30:587–98.
46. Factor VM, Kiss A, Woitach JT, Wirth PJ, Thorgeirsson SS. Disruption of redox homeostasis in the transforming growth factor-α/c-myc transgenic mouse model of accelerated hepatocarcinogenesis. J Biol Chem 1998;273:15846–53.
47. Calvisi DF, Ladu S, Hironaka K, Factor VM, Thorgeirsson SS. Vitamin E down-modulates iNOS and NADPH oxidase in c-Myc/TGF-α transgenic mouse model of liver cancer. J Hepatol 2004;41:815–22.
48. Bartsch H, Hietanen E, Malaveille C. Carcinogenic nitrosamines: free radical aspects of their action. Free Radic Biol Med 1989;7:637–44.
49. Bansal AK, Bansal M, Soni G, Bhatnagar D. Protective role of Vitamin E pre-treatment on N-nitrosodiethylamine induced oxidative stress in rat liver. Chem Biol Interact 2005;156:101–11.
50. Pereira MA. Chemoprevention of diethylnitrosamine-induced liver foci and hepatocellular adenomas in C3H mice. Anticancer Res 1995;15:1953–6.
51. Reliene R, Fischer E, Schiestl RH. Effect of N-acetyl cysteine on oxidative DNA damage and the frequency of DNA deletions in atm-deficient mice. Cancer Res 2004; 64:5148–53.
52. Sablina AA, Budanov AV, Ilyinskaya GV, Agapova LS, Kravchenko JE, Chumakov PM. The antioxidant function of the p53 tumor suppressor. Nat Med 2005;11: 1306–13.
53. Maeda S, Kamata H, Luo JL, Leffert H, Karin M. IKKβ couples hepatocyte death to cytokine-driven compensatory proliferation that promotes chemical hepatocarcinogenesis. Cell 2005;121:977–90.